

Article

Not peer-reviewed version

Development and Initial Validation of the Novel Computational Method for Dynamic Intracardiac Blood Flow Evaluation

[Dmytro Volkov](#)*, [Dmytro Skoryi](#)*, Bogdan Batsak, [Iurii Karpenko](#), Alamjeet Kaur Sidhu, [Carola Gianni](#)*, [Vincenzo Mirko La Fazia](#), [Bryan MacDonald](#), Joseph Gallinghouse, Rodney Horton, Sanghamitra Mohanty, Andrea Natale

Posted Date: 12 March 2026

doi: 10.20944/preprints202603.0955.v1

Keywords: intracardiac blood flow; turbulence; left atrium; atrial fibrillation; echocardiography; cardiac imaging



Preprints.org is a free multidisciplinary platform providing preprint service that is dedicated to making early versions of research outputs permanently available and citable. Preprints posted at Preprints.org appear in Web of Science, Crossref, Google Scholar, Scilit, Europe PMC.

Copyright: This open access article is published under a [Creative Commons CC BY 4.0 license](#), which permit the free download, distribution, and reuse, provided that the author and preprint are cited in any reuse.

Disclaimer/Publisher's Note: The statements, opinions, and data contained in all publications are solely those of the individual author(s) and contributor(s) and not of MDPI and/or the editor(s). MDPI and/or the editor(s) disclaim responsibility for any injury to people or property resulting from any ideas, methods, instructions, or products referred to in the content.

Article

Development and Initial Validation of the Novel Computational Method for Dynamic Intracardiac Blood Flow Evaluation

Dmytro Volkov ^{1,2,*}, Dmytro Skoryi ^{3,*}, Bogdan Batsak ⁴, Iurii Karpenko ⁵, Alamjeet Kaur Sidhu ⁶, Carola Gianni ¹, Vincenzo Mirko La Fazia ¹, Bryan MacDonald ¹, Joseph Gallinghouse ¹, Rodney Horton ¹, Sanghamitra Mohanty ¹ and Andrea Natale ^{1,7}

¹ Department of Electrophysiology, Texas Cardiac Arrhythmia Institute, St. David's Medical Center, Austin, TX, USA

² Neuron Medical, Brno, Czech Republic

³ Department of Innovation Engineering, Private Institution "University of Science, Entrepreneurship, and Technology"

⁴ University Clinic of Taras Shevchenko National University, Kyiv, Ukraine

⁵ Odessa National Medical University, Odessa, Ukraine

⁶ Kharkiv National Medical University, Kharkiv, Ukraine

⁷ Interventional Electrophysiology, Scripps Clinic, San Diego, CA, USA

* Correspondence: volkov@hearthealth.pro (D.V.); skoryidmytro@gmail.com (D.S.)

Abstract

Background/Objectives: To develop and preliminarily evaluate a practical Python-based program for universal dynamic intracardiac blood flow visualization and the extraction of new quantitative parameters, serving as an initial step toward future flow-based cardiac evaluation. **Methods:** The method was applied across five imaging modalities (angiography, MRI, ICE, TEE, TTE) using standard diagnostic hardware. Preliminary testing used ECG-gated ICE DICOM images from sixteen patients undergoing first-time AF ablation. **Results:** The program produced straightforward, easily adoptable flow visualizations and automatically computed the *Turbulence Index (TI)* and *Blood Mobility Fraction (BMF)* across cardiac cycles. Distinct preliminary flow patterns were observed between sinus rhythm and atrial fibrillation. Outputs are exportable for AI analysis. **Conclusions:** This approach demonstrates preliminary feasibility for simple, broadly applicable intracardiac flow assessment and introduces TI and BMF as promising flow-based biomarkers for future prognostic use.

Keywords: intracardiac blood flow; turbulence; left atrium; atrial fibrillation; echocardiography; cardiac imaging

1. Introduction

Atrial fibrillation (AF) is an increasingly prevalent global issue, with cases rising sharply in the USA and worldwide. While catheter ablation has become the most effective treatment, 20-30% of patients experience arrhythmia relapses requiring additional interventions [1]. Multi-modality imaging is crucial for predicting ablation success and determining adequate ablation volume [2]. Despite numerous studies and algorithms, accurately calculating thromboembolic risks associated with AF, ablation, cardioversion, and concomitant diseases remains challenging. Investigating and analyzing the blood flow in atrial chambers could provide valuable insights and address gaps in our understanding of AF pathophysiology [3,4]. Historical and theoretical background on blood flow estimation is provided in S1.

Potential-kinetic energy interchange during flow and blood kinetic energy are crucial, with many measurements and indices describing kinetic energy changes using vector flow mapping and contrast echocardiography via particle image velocimetry [12,13]. Turbulence, with its own features, is an unavoidable result of viscosity during blood propulsion and is connected to blood velocity and kinetic energy. Effects of turbulence can be dynamically traced, measured, and analyzed as an independent factor of blood flow efficiency via different imaging modalities [14,15]. Additionally, calculating energetically different blood pools within the chambers is important for assessing cardiac function and prognosis [17]. Recent advancements in blood flow evaluation and calculations offer new prospects for determining multivariate prognoses, including heart failure and stroke [18,19].

Like other chambers, LA flow has been investigated in several studies using contrast TTE and MRI tools. These studies generate various parameters depicting LA flow, with a focus on flow vortex formation and its evaluation as a crucial aspect of blood flow behavior [20–22]. Despite significant efforts from multiple scientific groups, a clear understanding of the complex physiological and pathological mechanisms of intracardiac flow remains elusive, particularly in terms of simplified numeric indices. The current study aims to address this gap in a small cohort of patients undergoing their first AF ablation (S2).

2. Materials and Methods

As blood flows through cardiac chambers, it inevitably creates some level of turbulence and different moving blood patterns. Visual surrogates of those physical phenomena can be obtained with various radiological diagnostic equipment by special enhancement and digitally represented by dynamic changes of the blood particle dimensions and their fractal characteristics (Figure 1 a-c).

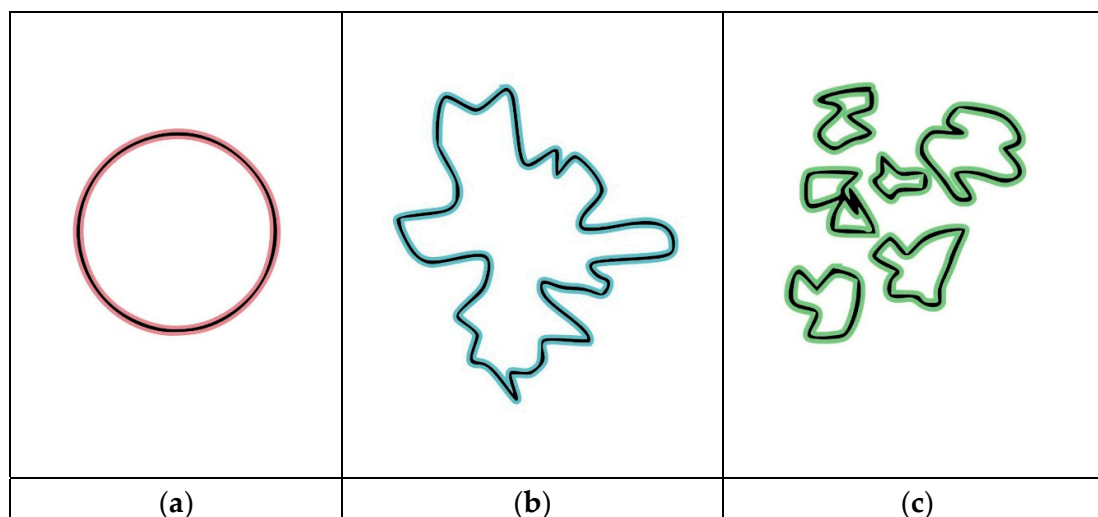


Figure 1. Schematic representation of the different fractal states of moving blood particles as a visual surrogate for turbulence levels: (a) a round-shaped object; (b) a fractal surface object; and (c) disintegration into several highly fractalized separate objects.

The application of a specific dynamic subtraction mode to analyze blood flow patterns through continuous digital evaluation of the rate and degree of blood pool fragmentation is one of the core concepts of the proposed technology. The dynamically subtracted frames are created by calculating the difference in pixel brightness between corresponding points in two consecutive frames. The resulting image represents the grayscale level of the displacement vector amplitude, where black and white indicate the most movable areas, and gray indicates the most stable. A series (cine loop) of these dynamically subtracted frames was used to identify the 'bright' actively moving components and the gray passively pooling components, which were further separated into several groups according to their intensity (i.e., isophotes) to emphasize dynamic blood flow changes [18].

A Python-based multiplatform desktop application was developed for the visual representation, extraction, and analysis of dynamic blood flow information, as well as outcome analysis in graphical and text formats. The application processes DICOM files containing image sets and corresponding ECG data from ultrasound, MRI, or angiographic sources. The image set is displayed in the application interface, allowing users to delineate ROI for cardiac cavity and wall segmentation. ROI delineation was performed dynamically, with manual adjustments if necessary, applied to each frame throughout the selected frame series for analysis (Figure S1).

The timing of the calculation window is selected based on the ECG strip and can include a defined number of consecutive cycles. Differential frames are then generated by dynamically subtracting two consecutive frames [23]. The resulting image is used to extract grayscale zones (isophotes) with equal intensity ranges for segmentation, color coding, and presentation in per-frame or cine mode. Additionally, the pixel-level cutoff can be determined (e.g., 200 pixels) (Figure 2 a-f).

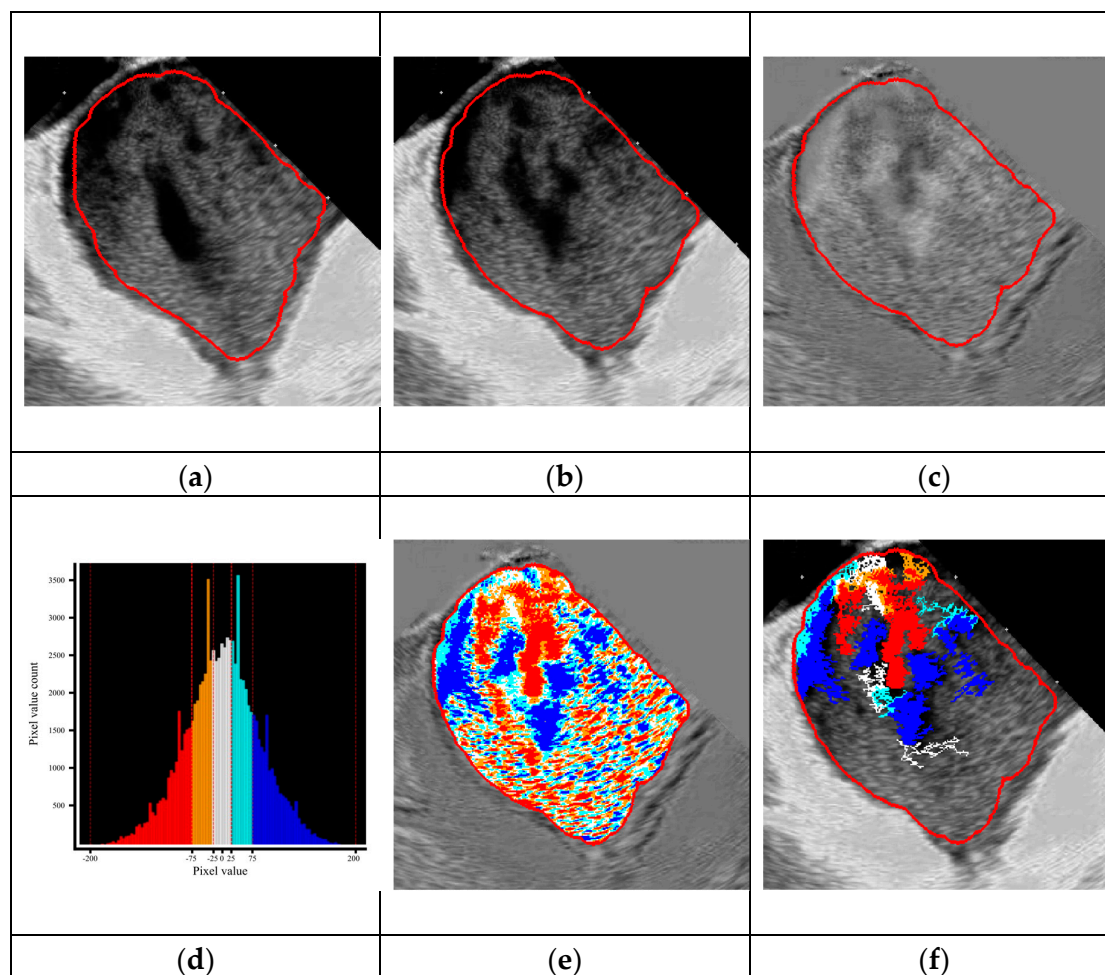


Figure 2. The main algorithm of the raw data elaboration on the example of ICE-derived LA flow: dynamic continuous subtraction of the predefined ROI of two consecutive native frames (a-b) with the generate on of a differential frame (c); color coding of differential frames by dedicated gray scaling (d) into 5 color layers (e); programmed pixel cutoff level (200 pixels) to determine the proportion of the pixel size presence above the cutoff (f).

The program has several workflow steps: 1) dynamic subtraction of two consecutive native images; 2) generation of series of dynamically subtracted frames; 3) color coding of the obtained gray spectrum in five layers; 4) dynamic visualization of the blood flow by choosing active layers; 5) determination of pixels area withdrawal to filter blood particles dimensions; 6) TI and BMF calculation and numeric and graphical representation; and 7) digital data export.

Two new indices of intracardiac blood flow were proposed:

- Turbulence index (TI) - fractality level of the different blood pools;
- Blood mobility fraction (BMF) - pixel dimensions coding of the moving blood particles.

Certain formulas and approaches were used to implement the program's algorithms and calculate indices, including creation of the isophote level intervals to structure the image (S3), TI calculations (S4), and BMF calculations (S5).

The current program version limits the number of isophote layers to five, based on grayscale intensity (red and violet - marginal; orange and blue - medial; white - median). The original TI calculation is the relative ratio of the actual pixel contour length to the minimal possible perimeter of a circle with the same area [23]. The program performs both aggregative and layer-based calculations to assess the distribution of isophotes, their absolute area in pixels, their relative area compared to other isophotes, and the overall ROI. It also tracks changes in these parameters per frame, along with overall TI and its per-frame variations. Additionally, the program includes all levels of isophotes for processing, depending on their absolute area in pixels, by establishing a cutoff isophote area threshold. The BMF is calculated as the percentage of the summed pixel area after cutoff relative to the total ROI, representing the most active, "movable" blood clusters. The program's algorithm flowchart is presented in Figure S2. The program's working window is presented in Figure S3.

The observation of smaller square particles during impaired LA flow, possibly representing pooling blood segments, led to the idea of calculating blood particle pixel size as a marker of hemodynamic effectiveness. A higher relative percentage of larger pixel sizes was associated with more active flow, termed blood mobility fraction (BMF). Cutting off smaller pixel size isophotes can enhance blood flow visualization and reduce echo noise (Figure 3).

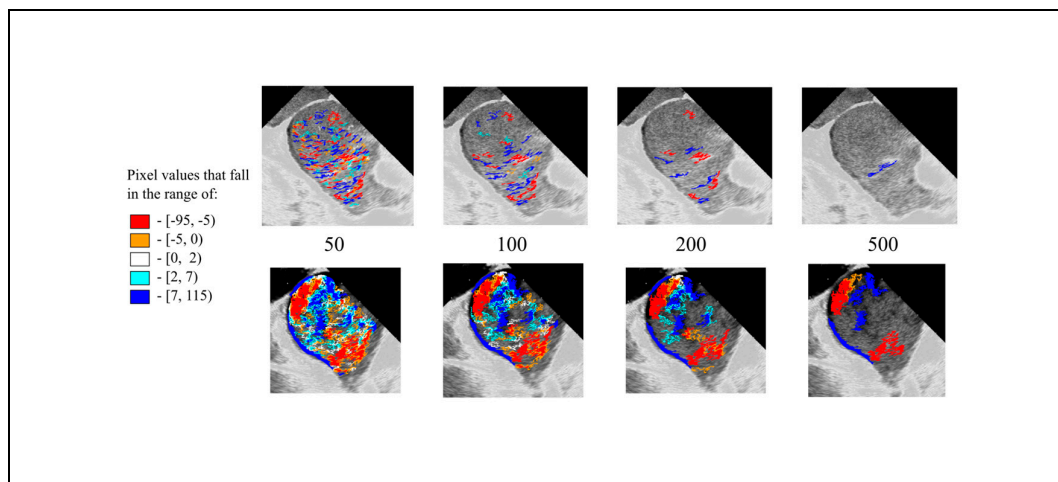


Figure 3. Visual representation of the conduit LA phase in persistent AF (upper row) and paroxysmal AF with SR patient (bottom row) by incremental pixel cut-off (50-100-200-500).

16 patients (age 66.9 ± 15.2) with first elected AF ablation procedure (paroxysmal - 8 (female - 2), persistent - 8 (female - 4)) were included into the current study. Main basal clinical and instrumental data of the patients are presented in Table 1.

Table 1. Intraprocedural data of the patients.

Patients, n=16	Paroxysmal AF, n=8	Persistent AF, n=8	p-value
Age	59±19	74±8	0.0551
BMI	26.4	29.3	0.1856
CHA2DS2-VASC score	2.0	3.9	0.0205

LVEF, %	58±7	60±10	0.5971
LA dimensions, mm	40±3.8	43±3.6	0.0523
Mitral max velocity, m/s	0.66±0.25	0.89±0.36	0.0657
Mitral deceleration, ms	198±35	183±28	0.5619
MR, grade	1.1±0.4	1.4±0.7	0.1108

Patients with persistent AF were older, had obesity, more dilated LA, higher grade of MR and CHA2DS2VASc score.

All the patients underwent successful uneventful PVI, roof line and PWI, except one patient of 26 yo, with PVI only. CTI line was done in 2 patients with coexisted typical atrial flutter. All the patients received uninterrupted direct anticoagulation and were in the therapeutic range of ACT throughout the procedure.

Pulsed wave and color Doppler images of PV and transmitral flow were recorded to characterize the flow and calculate velocities. Prucka EP system was used ECG measurements. Intraprocedural data are shown in Table 2.

Table 2. Demographic and clinical characteristics of the patients.

Patients	Paroxysmal AF, n=8	Persistent AF, n=8	p-value
ECG with SR			
HR, bpm	62±15	70±17	0.5287
P wave, ms	106±15	104±17	0.7948
PR, ms	151±30	158±23	0.6383
QRS, ms	97±26	90±21	0.5287
QT, ms	412±56	397±45	0.9601
Peak velocities (ICE), m/s			
LAA	0.48±0.13	0.3±0.11	0.0106
Left PVs	0.47±0.15	0.36±0.06	0.0929
Right PVs	0.31±0.16	0.4±0.18	0.0404
Transmitral flow	0.46±0.07	0.58±0.1	0.0209
Mean LA pressure	13±5	19±7	0.0930

Patients in the persistent group had significantly lower peak velocities in LAA, but higher in RPV and transmitral flow.

ICE ECG-gated Dicom images were recorded by Acunav Acuson probes from RA position on Siemens 2000 echo machine throughout the procedure. A default frame rate of 80-90 per second and increased gain of 20 was implemented to enhance flow visualization. Then Dicom files were used for the offline calculation by the program. Three consecutive ECG-gated cardiac cycles were analyzed. As a result, enhanced color-coded visual representation of LA blood flow was outlined and digital graphs of dynamic TI and pixel number dependent particles square distribution were created in ECG-gated LA intervals framework. Obtained color coded flow information as well as general charts' patterns were delineated visually and by digital comparison of dynamic TI values and average, maximal and minimal BMF under different pixel cut-off (50-1200).

Continuous variables are reported as mean \pm standard deviation. Categorical variables are reported as counts and percent. Continuous variables were compared using Mann-Whitney U test or independent samples t test, dependent on their distribution. Chi-square test was used to compare categorical variable between the groups. All the tests were two-tailed and conducted at an α level of 0.05. Statistical analysis was performed with SPSS statistics for Windows 25 (IBM, Armonk, New York, United states).

3. Results

3.1. Visual Representations of the Flow Patterns

The program has the potential to provide dynamic whole-chamber visualization of blood flow behavior throughout several cardiac cycles (Figure S4,) and subsequently use that information for parameter calculations.

The program was successfully applied in several radiological modalities (Figure S5).

The visual effects and patterns of flow created by software are extremely complex and cannot be directly classified into distinct subtypes, but even in 2D environment the program gives visual enhancement of tracing the main features of the flow including vortexes formation (Figure S6). Nonetheless, as two main types of vortexes along with parallel flow exist in classic fluid mechanics, links of actual LA flow to those three models have been attempted. The impaired flow patterns were comparable to those of rigid-body-like vortexes (rotational), which are, by definition, more stable, difficult to change within the cardiac cycle and need additional energy to support their flow. This usually coincided with mild LA walls contraction and advanced visual dissynchrony. To some extent, this type of flow was present in all patients with sustained AF, as indicated by slow, equal-velocity circumflex movement of the blood inside the LA. In contrast, the free vortex (irrotational), which saves initial energy within the vortex, was linked to more visually active flow in patients with initial SR, active synchronous LA wall contraction and often during flow facilitation under isoprenaline infusion. Parallel flow was present in the regions of severe akinetic LA because of brisk inward PV flow into the almost completely stuck and unguided LA blood pool with further slow progression and dissipation. In the worst-case scenario, the flow looked chaotic due to the short-living, small unpredictable push of blood, with a significant part of the wave-like parallel flow patterns, which is theoretically attributed to the highest stress shear forces (Figure 4 a-c).

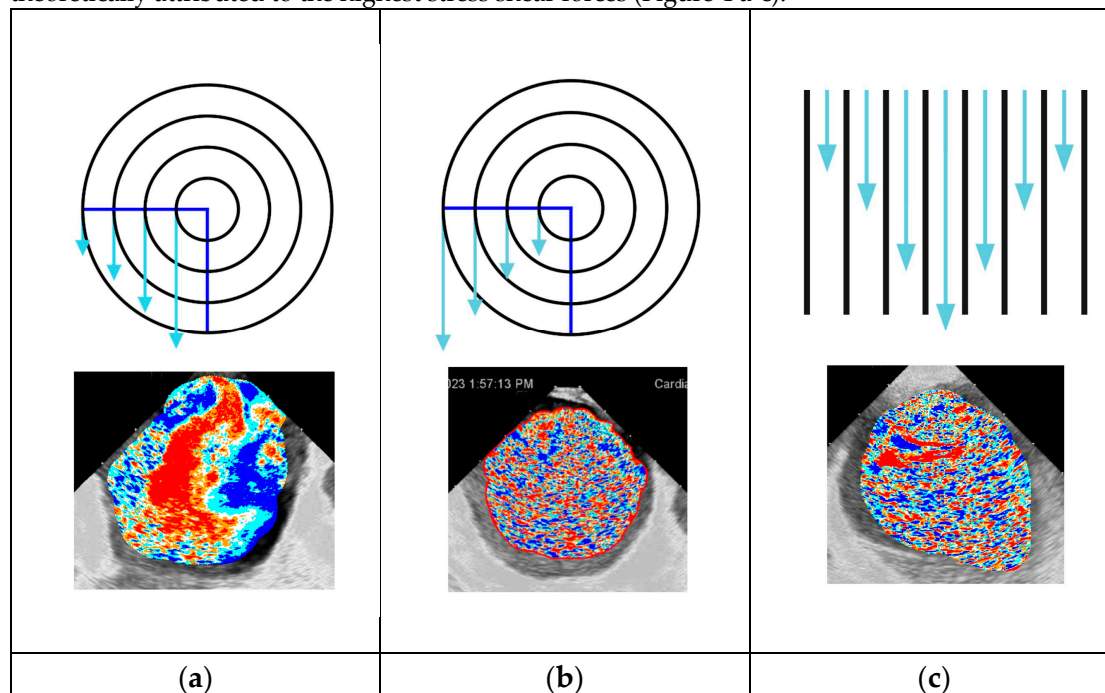


Figure 4. Schematic representation and actual examples of the physical patterns of the (a) irrotational, (b) rotational vortices and (c) parallel flow in different patients (Video S 1 a-c).

One more obvious visual conclusion has been made—more active flow in patients with SR and paroxysmal AF was expressed by the larger relative isophote area with active behavior and closer interconnection between isophote clusters. The marginal forms of isophotes were surrounded by medial forms with a thin white median color layer between those groups, indicating the engagement of more passive blood pools by incoming blood flow. In contrast, patients with persistent AF had more stable, chaotic, and slower flow evolution, ranging from unstable restricted area vortices and sometimes consistent whole-chamber slow-moving circles (rotational vortices) to straight and elliptical, extremely slowly progressing long waves crossing the part of the chamber to become stale without any vortex formation.

These phenomena were inherent to the different ICE projections, including a more anterior LA view closer to the MV with visualization of vortex progression toward the LV, and the contraction pattern of the atrial walls could also be retrieved (Figure 5 a-d).

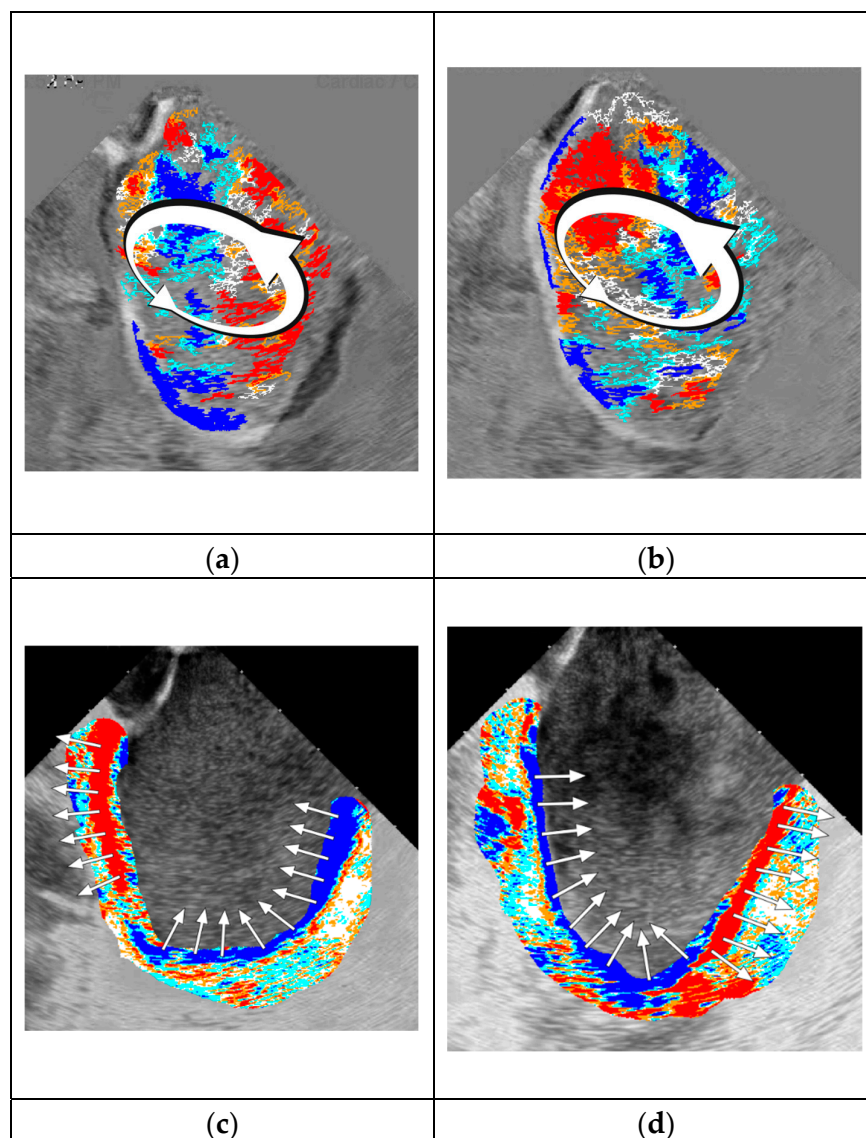


Figure 5. Descending vortex progression parallel to the plane of the MV: (a, b) two consecutive frames representing the CCW vortex; (c, d) program color coding of LA walls contraction with obvious dissynchrony in both opposite phases of the cardiac cycle facilitating the rotational nature of the vortex (Video S 2 a, b).

3.2. Program-Derived Data Repetitiveness and Correlation with Cardiac Cycle Phases and Other Parameters

Program evaluation of ICE-derived data revealed repetitive phased atrial patterns of TI and BMF within up to 30 consecutive cardiac cycles in patients with a stable-rate SR and preserved atrial mechanical function presented on Figure 6 (a-d).

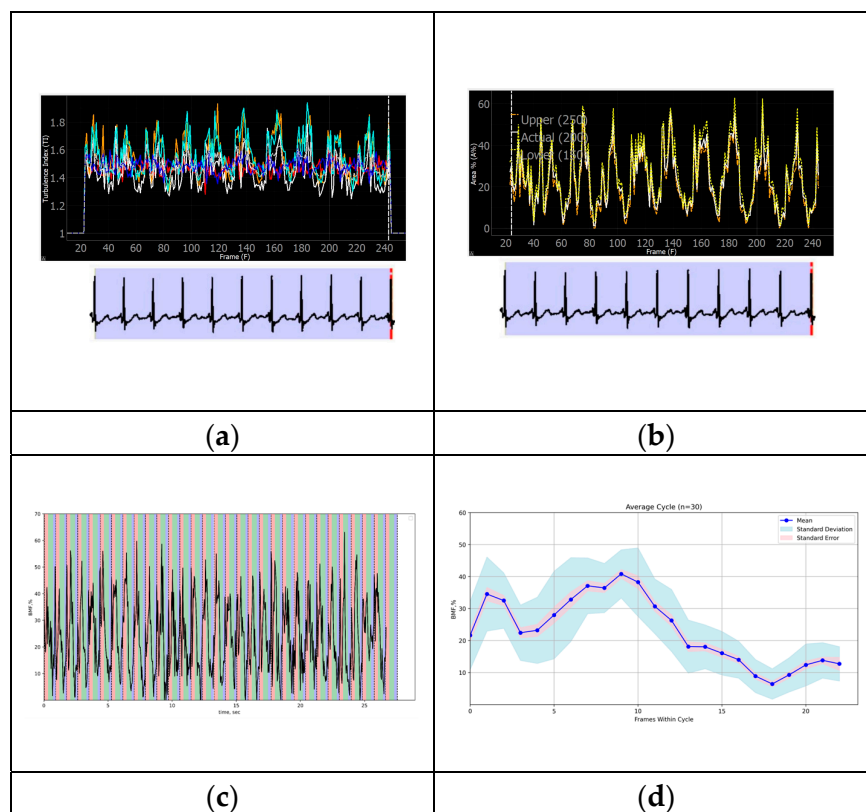


Figure 6. Reproducible program patterns of TI and BMF (200) based on atrial ICE images: (a) TI curve and (b) BMF curve; (c) BMF curve of 30 cardiac cycles relative to the reservoir (red), conduit (green) and booster (blue) atrial phases — in addition to cardiac cycle-dependent changes, respiratory fluctuations of the curve can be registered; (d) BMF distribution during the average cycle of 30 consecutive cardiac cycles with standard deviation and standard error relations.

Moreover, geometry of BMF curves, for instance, can be distinguished between different atrial pacing sites reflecting possibly dyssynchronous and alternating blood flow formation in specific circumstances including cardiac pacing. TI and BMF curves findings are included in the S6.

3.3. Comparison of the Blood Flow Patterns Among Study Patients' Groups

In general, patients with persistent AF exhibited less active and more disorganized blood flow patterns compared to those with paroxysmal AF in SR. Comparative data of BMF of 200 pixels presented in Table 3.

Table 3. Maximum, minimum and range BMF 200 values in the study groups.

Patients	BMF Maximum value		BMF Minimum value		BMF Min-Max range	
	PesrAF	PAF	PesrAF	PAF	PersAF	PAF
1	15.4	41.8	2.8	5.8	12.6	36
2	17.9	16.3	1.28	0.5	16.6	15.8
3	8.4	30.4	2.7	2.4	5.7	28
4	19.6	21.9	2.4	0	17.2	21.9
5	14.2	78.6	3	1.6	11.2	77

6	9.1	15.9	2.2	0.9	6.9	15
7	8.7	18.7	1.8	1.9	7	16.8
8	29.3	25.1	0.5	3.1	28.8	22
Avg	15.3	31.1	2.1	2	13.3	29.1
SD	7.1	21	0.8	1.8	7.7	20.6
p-value	0.0238		0.6383		0.0315	

The paroxysmal group presents statistically higher maximal BMF 200 values and a greater range between maximal and minimal BMF, indicating more active dynamic flow changes connected to LA phases. Minimal BMF values were comparable between both groups.

Patients in the paroxysmal group had higher average BMF across all cutoff levels, (Figure 7 a-d).

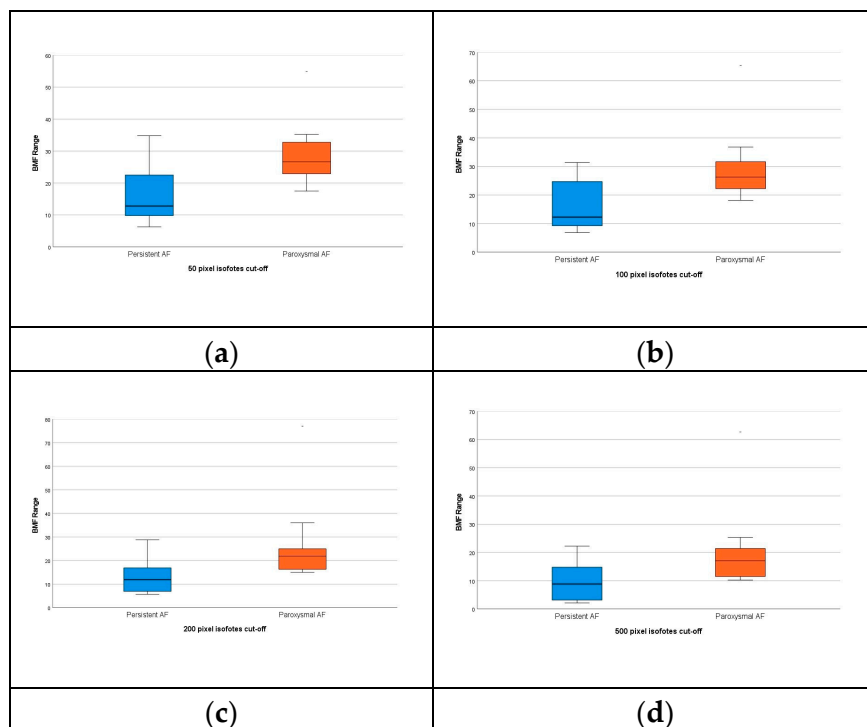


Figure 7. Comparison of different pixel leveled (50-100-200-500) average BMF between groups with paroxysmal and persistent AF represents statistically higher BMF values in the paroxysmal group.

A visual and graphical analysis of the program performance of two selected patients with paroxysmal AF in the SR (m, 26; BMI - 26.1; CHA2DS2-VASC - 0) and persistent AF (m, 73; BMI - 30.7; CHA2DS2-VASC - 5) are presented on Figure 8 (a, b).

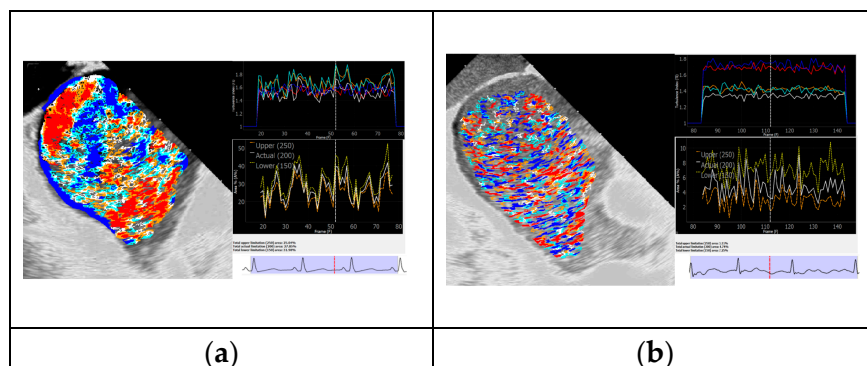


Figure 8. Comparison of visual and graphical blood flow representations in selected patients with SR (a) and AF (b) from the groups.

The abovementioned patients presented obviously different visual flow pictures as well as TI and BMF curves. The TI curve in patients with persistent AF was presented as a low-amplitude rigid separated lines, and the BMF had chaotic deviations and a low absolute maximum and range values. In contrast, the SR patients had more dynamic and synchronized TI and BMF curves, clear connections to the cardiac cycle phases, and several times greater BMF values (BMF (200) 28% vs 5%, respectively, for the presented comparison).

Further analysis of the patients with an incremental pixel cutoff of up to 1200 revealed obviously different graphical representations of the LA flow characteristics, as shown in Figure 9.

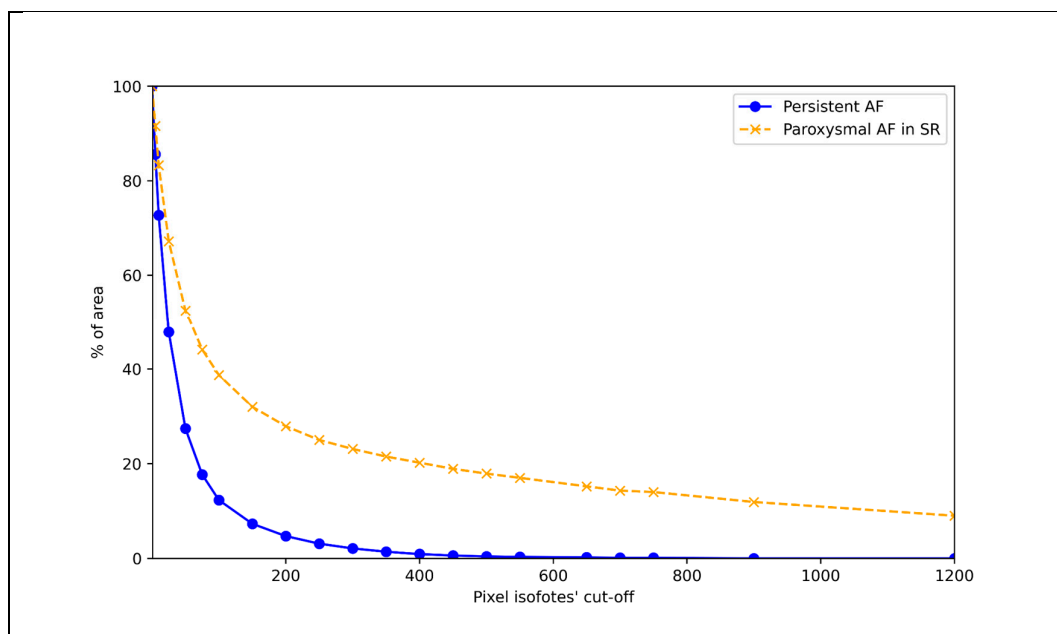


Figure 9. Graphical distribution of max. BMF with incremental pixel cutoff in two selected patients from the persistent and paroxysmal AF groups.

4. Discussion

Our understanding of cardiac blood flow dynamics has advanced significantly, but many aspects remain to be elucidated, especially considering blood flow as a key indicator of electro-mechanical efficiency. Some researchers suggest that evaluating blood flow might offer more precise prognostic value than merely tracing cardiac wall displacements [17].

Understanding diverse blood flow patterns and developing new, digitalized indices of dynamic intracardiac blood flow are crucial in the era of personalized medicine, advanced technology, and machine learning revolution. A dynamic, color-Doppler-like tool applicable to whole-chamber visualization would be valuable to various specialists [11]. Providing digitized information alongside traditional views, especially in a straightforward numeric format, enhances its utility. On the other hand, such a derivative approach can generate specific data sets amenable for AI.

To our knowledge, this study is the first to use ICE-guided, non-contrast imaging for dynamic, whole-chamber flow visualization, evaluating and calculating new parameters of flow efficiency aligned with established clinical standards.

The program's visualization of blood flow revealed its vortex-like nature in the LA, influenced by patients' rhythm and medical history, consistent with previous studies on cardiac chamber flow [24,25]. However, while vortex formation is a significant observation, it does not ensure an adequate

flow pattern. Various types of vortices exist, and despite the development of specific indices to characterize them, these are not yet widely adopted by cardiologists.

Historically, echocardiographic imaging of blood flow has relied on echo-contrast agents to enhance visibility, or on high-frame-rate probes for non-contrast acquisition [26,27]. The proposed approach, utilizing native loops and standard probes, appears more feasible for routine application.

Despite years of worldwide CHA2DS2-VASC score adaptation, questions still exist about the additional parameters not considered in the algorithm including blood flow characteristics itself and factors that directly influence it [28]. Some authors pointed out that LA structural features and connected flow beyond LAA may affect stroke risk, especially subclinical events [16,18]. There are conflicting data about MR as the additional modifying factor of LA thrombus formation, as higher grade of MR may facilitate the flow and decrease that probability [29,30]. Calculating LA flow could fill up this potential gap and be used as the missing point of CHA2DS2-VASC score [31,32]. This could enhance thromboembolic risk stratification by digitally quantifying “smoke” effect not only in LAA, but in LA itself.

We acknowledge that this first study to preliminary validate the new approach and test the software has clear technical, clinical and statistical limitations. As with any echocardiographic method, image quality dependence is a primary technological concern that can influence results. To ensure consistency, we used images retrieved from the same model of echo machine (Siemens SC 2000) with predefined, similar settings. However, extending this technology to different hardware would require calibration and additional testing. The flow was primarily calculated in single-plane 2D models, which are inherently less accurate than 3D environments, so transitioning from pixel- to voxel-derived calculations could be the next step. Additionally, blood viscosity, an important factor in turbulence, was not accounted for in the calculations.

The study was conducted on a small cohort of patients without a comparison group of healthy individuals, limiting the ability to define normal values for the proposed indices. Further research is needed, including statistically justified studies based on a broader range of clinical markers and extended follow-up with corresponding outcomes in a larger patient cohort. Such studies will help further validate the clinical efficacy of the proposed method, refine the proposed indices, and explore the potential role of AI in data analysis (S7).

5. Conclusions

1. A Python-based computer program was created to specifically analyze the cyclic intracardiac blood flow phenomena with the focus on the visual surrogates of the turbulence digital calculations.
2. The program creates enhanced dynamic color-coded whole chamber visualization of intracardiac blood flow using regular raw radiological data inputs from conventional hardware via different imaging modalities.
3. The newly proposed TI and BMF were preliminary validated on a small dataset of ICE images as special dynamic indices of blood flow evaluation and had recognizable patterns in selected SR and AF patients.

6. Patents

Patent US 10,631,811 B2, United States Patent; A61B6/032, A61B8/06, A61B8/0883 Method and system for processing of medical images for generating of prognosis of cardiac function. Dmytro Volkov, Valerij Boyko, Alexander Bakai; appl. No 15/060,970; filed 04.03.2016; issued 28.04.2020.

Supplementary Materials: The following supporting information can be downloaded at website of this paper posted on Preprints.org.

Author Contributions: Dmytro Volkov: Conceptualization, Data curation, Methodology, Project administration, Software Validation, Writing – original draft. Dmytro Skoryi: Resources, Software, Visualization. Bogdan Batsak:

Conceptualization, Software, Visualization. Iurii Karpenko: Conceptualization, Resources. Sidhu Alamjeet Kaur: Data curation, Formal analysis. Carola Gianni: Data curation, Methodology, Validation. Vincenzo Mirko La Fazia: Formal analysis, Investigation. Bryan MacDonald: Data curation, Formal analysis, Investigation. G. Joseph Gallinghouse: Data curation, Investigation. Rodney Horton: Methodology, Project administration, Supervision. Sanghamitra Mohanty: Investigation, Methodology, Supervision. Andrea Natale: Conceptualization, Methodology, Project administration, Supervision.

Funding: This research received no external funding.

Institutional Review Board Statement: The patients' dataset was collected as part of the clinical database of patients undergoing electrophysiology procedures at St. David's Medical Center in Austin, Texas, United States (St. David's HealthCare IRB #18-05-07).

Informed Consent Statement: Data for this study were obtained from a prospective clinical database of recorded cases at St. David's Medical Center (Austin, TX, USA). All records were fully de-identified prior to analysis to ensure patient privacy. The study was conducted under the framework of the institutional database protocol (IRB #18-05-07), and because the research involved only secondary analysis of anonymized data, it was exempt from further institutional review. Patient consent was waived due to the use of a completely de-identified dataset of recorded cases where no protected health information (PHI) was accessible to the researchers.

Data Availability Statement: Data, including raw data, methods, protocols, and software, will be made available on argued request. For requesting data, please write to the corresponding author.

Conflicts of Interest: Dmytro Volkov received non-provisional USA Patent for the part of the technology described in the article [23]. The authors declare that they have no known competing financial interests or personal relationships that could have appeared to influence the work reported in this paper.

Abbreviations

The following abbreviations are used in this manuscript:

AF	Atrial fibrillation
AI	Artificial intelligence
BMF (n)	Blood mobility fraction with n-pixel cutoff
CW	Clockwise
CCW	Counterclockwise
ECG	Electrocardiogram
ICE	Intracardiac echocardiography
LA	Left atrium, left atrial
LAA	Left atrial appendage
LV	Left ventricle, left ventricular
MR	Mitral regurgitation
MRI	Magnetic resonance imaging
PAF	Paroxysmal AF
PersAF	Persistent AF
PV(s)	Pulmonary vein(s)
RA	Right atrium, right atrial
ROI	Region of interest
TI	Turbulence index
TTE	Transthoracic echocardiography
TEE	Transesophageal echocardiography
TR	Tricuspid regurgitation

References

1. January CT, Wann LS, Calkins H, Chen LY, Cigarroa JE, Cleveland JC Jr, Ellinor PT, Ezekowitz MD, Field ME, Furie KL, Heidenreich PA, Murray KT, Shea JB, Tracy CM, Yancy CW. 2019 AHA/ACC/HRS Focused Update of the 2014 AHA/ACC/HRS Guideline for the Management of Patients With Atrial

- Fibrillation: A Report of the American College of Cardiology/American Heart Association Task Force on Clinical Practice Guidelines and the Heart Rhythm Society in Collaboration With the Society of Thoracic Surgeons. *Circulation*. 2019;140(2):e125-e151.
2. E, Lip GY, Galderisi M, Goette A, Shah D, Marwan M, Lederlin M, Mondillo S, Edvardsen T, Sitges M, Grapsa J, Garbi M, Senior R, Gimelli A, Potpara TS, Van Gelder IC, Gorenek B, Mabo P, Lancellotti P, Kuck KH, Popescu BA, Hindricks G, Habib G, Cardim NM, Cosyns B, Delgado V, Haugaa KH, Muraru D, Nieman K, Boriani G, Cohen A. EACVI/EHRA Expert Consensus Document on the role of multi-modality imaging for the evaluation of patients with atrial fibrillation. *Eur Heart J Cardiovasc Imaging*. 2016;17(4):355-83.
 3. Bosi GM, Cook A, Rai R, Menezes LJ, Schievano S, Torii R, Burriesci G Burriesci. Computational Fluid Dynamic Analysis of the Left Atrial Appendage to Predict Thrombosis Risk. *Front Cardiovasc Med*. 2018;5:34.
 4. Spartera M, Pessoa-Amorim G, Stracquadanio A, Von Ende A, Fletcher A, Manley Pet al. Left atrial 4D flow cardiovascular magnetic resonance: a reproducibility study in sinus rhythm and atrial fibrillation. *J Cardiovasc Magn Reson*. 2021;23:29.
 5. Klabunde RE. *Cardiovascular physiology concepts*. PA: LWW, 3d edition, 2021, 272p.
 6. K. Kundu, Ira M. Cohen and David R. Dowling. *Fluid Mechanics*. 6th Edition. Elsevier Inc. 2016. 784p.
 7. Kaufmann TAS, Graefe R, Hormes M, Schmitz-Rode T, Steinseiferand U. *Computational Fluid Dynamics: Theory, Analysis and Applications*. P. 109–136.
 8. Baillargeon B, Rebelo N, Fox DD., Taylor RL, Kuhl E. The Living Heart Project: A robust and integrative simulator for human heart function. *European Journal of Mechanics - A/Solids*. 2014;48:38-47.
 9. Qin JJ, Indja B, Gholipour A, Gök M, Grieve SM. Evaluation of Left Ventricular Function Using Four-Dimensional Flow Cardiovascular Magnetic Resonance: A Systematic Review. *J Cardiovasc Dev Dis*. 2022;9(9):304.
 10. Dyverfeldt P, Bissell M, Barker AJ, Bolger AF, Carlhäll CJ, Ebbers T, Francios CJ, Frydrychowicz A, Geiger J, Giese D, Hope MD, Kilner PJ, Kozerke S, Myerson S, Neubauer S, Wieben O, Markl M. 4D flow cardiovascular magnetic resonance consensus statement. *J Cardiovasc Magn Reson*. 2015;17(1):72.
 11. Fiorencis A, Pepe M, Smarrazzo V, Martini M, Severino S, Pergola V, Evangelista M, Incarnato P, Previtiero M, Maglione M, Iliceto S, Pedrizzetti G, Mele D. Noninvasive Evaluation of Intraventricular Flow Dynamics by the HyperDoppler Technique: First Application to Normal Subjects, Athletes, and Patients with Heart Failure. *J Clin Med*. 2022;11(8):2216.
 12. GR, Kim M, Pedrizzetti G, Vannan MA. Current clinical application of intracardiac flow analysis using echocardiography. *J Cardiovasc Ultrasound*. 2013;21(4):155-62.
 13. D, Beccari R, Pedrizzetti G. Effect of Aging on Intraventricular Kinetic Energy and Energy Dissipation. *J Cardiovasc Dev Dis*. 2023;10(7):308.
 14. J, Eriksson J, Dyverfeldt P, Bolger AF, Ebbers T, Carlhäll CJ. Turbulent kinetic energy in normal and myopathic left ventricles. *J Magn Reson Imaging*. 2015;41(4):1021-9.
 15. Volkov D, Batsak B, Skoryi D. Blood flow turbulence index as a new parameter for cardiac function assessment in various cardiac imaging modalities. *European Journal Of Heart Failure*. 2022;24:84-85.
 16. Bäck S, Skoda I, Lantz J, Henriksson L, Karlsson LO, Persson A, Carlhäll CJ, Ebbers T. Elevated atrial blood stasis in paroxysmal atrial fibrillation during sinus rhythm: a patient-specific computational fluid dynamics study. *Front Cardiovasc Med*. 2023;10:1219021.
 17. D, Trevisan F, Fiorencis A, Smarrazzo V, Bertini M, Ferrari R. Current Role of Echocardiography in Cardiac Resynchronization Therapy: from Cardiac Mechanics to Flow Dynamics Analysis. *Curr Heart Fail Rep*. 2020;17(6):384-396.
 18. C, Jin Z, Liu R, Iwata S, Tugcu A, Yoshita Met al. LA volumes and reservoir function are associated with subclinical cerebrovascular disease: the CABL (Cardiovascular Abnormalities and Brain Lesions) study. *JACC Cardiovasc Imaging* 2013;6:313–23.
 19. Fyrenius A, Wigström L, Ebbers T, Karlsson M, Engvall J, BolgerAF. Three dimensional flow in the human left atrium. *Heart* 2001;86:448-55.

20. Park KH, Son JW, Park WJ, Lee SH, Kim U, Park JS, Shin DG, Kim YJ, Choi JH, Houle H, Vannan MA, Hong GR. Characterization of the left atrial vortex flow by two-dimensional transesophageal contrast echocardiography using particle image velocimetry. *Ultrasound Med Biol* 2013;39:62-71.
21. J, Gupta V, Henriksson L, Karlsson M, Persson A, Carlhäll CJ, Ebbers T. Impact of Pulmonary Venous Inflow on Cardiac Flow Simulations: Comparison with In Vivo 4D Flow MRI. *Ann Biomed Eng*. 2019;47(2):413-424.
22. Jingquan Z, Deyong L, Huimin C, Hua F, Xuebin H, Chenyang J, Yan L, Xuebin L, Min T, Zulu W, Yumei X, Jinlin Z, Wei Z, Xiaochun Z, Daxin Z, Yun Z, Changsheng M, Zei PC, Di Biase L. Intracardiac echocardiography Chinese expert consensus. *Front Cardiovasc Med*. 2022;9:1012731.
23. US 10,631,811 B2, United States Patent; A61B6/032, A61B8/06, A61B8/0883 Method and system for processing of medical images for generating of prognosis of cardiac function. Dmytro Volkov, Valerij Boyko, Alexander Bakai; appl. No 15/060,970; filed 04.03.2016; issued 28.04.2020.
24. Pedrizzetti G, La Canna G, Alfieri O. et al. The vortex - an early predictor of cardiovascular outcome? *Nat Rev Cardiol*. 2014;11:545-553.
25. Spartera M, Stracquadanio A, Pessoa-Amorim G, Von Ende A, Fletcher A, Manley P, Ferreira VM, Hess AT, Hopewell JC, Neubauer S, Wijesurendra RS, Casadei B. The impact of atrial fibrillation and stroke risk factors on left atrial blood flow characteristics. *Eur Heart J Cardiovasc Imaging*. 2021;23(1):115-123.
26. Cimino S, G. Pedrizzetti, G. Tonti, E. Canali, V. Petronilli, L. De Luca, C. Iacoboni, L. Agati. In vivo analysis of intraventricular fluid dynamics in healthy hearts. *European Journal of Mechanics - B/Fluids*. 2012;35:40-46.
27. Fadnes S, Wiggen MS, Nyrnes SA, Lovstakken L. In Vivo Intracardiac Vector Flow Imaging Using Phased Array Transducers for Pediatric Cardiology. *IEEE Transactions On Ultrasonics, Ferroelectrics, And Frequency Control*. 2017;64(9):1318-26.
28. Sun Y, Ling Y, Chen Z, Wang Z, Li T, Tong Q, Qian Y. Finding low CHA2DS2-VASc scores unreliable? Why not give morphological and hemodynamic methods a try? *Front Cardiovasc Med*. 2023 Jan 4;9:1032736.
29. Nakagami H, Yamamoto K, Ikeda U, Mitsuhashi T, Goto T, Shimada K. Mitral regurgitation reduces the risk of stroke in patients with nonrheumatic atrial fibrillation. *Am Heart J*. 1998;136:528-32.
30. Melduni R, Nkomo VT, Wysokinski W, Gersh BJ, Deshmukh A, Padang R, Greene EL, Oh JK, Lee HC. Risk of left atrial appendage thrombus and stroke in patients with atrial fibrillation and mitral regurgitation. *Heart*. 2022;108(1):29-36.
31. Van Laer SL, Verreyen S, Winkler KM, Miljoen H, Sarkozy A, Heuten H, Saenen J, Van Herck P, Van de Heyning CM, Heidebuechel H, Claeys MJ. Effect of Mitral Regurgitation on Thrombotic Risk in Patients With Nonrheumatic Atrial Fibrillation: A New CHA2DS2-VASc Score Risk Modifier? *Am J Cardiol*. 2021;145:69-76.
32. Spartera M, Stracquadanio A, Pessoa-Amorim G, Von Ende A, Fletcher A, Manley P, Ferreira VM, Hess AT, Hopewell JC, Neubauer S, Wijesurendra RS, Casadei B. The impact of atrial fibrillation and stroke risk factors on left atrial blood flow characteristics. *European Heart Journal - Cardiovascular Imaging*. 2022;23:115-123.

Disclaimer/Publisher's Note: The statements, opinions and data contained in all publications are solely those of the individual author(s) and contributor(s) and not of MDPI and/or the editor(s). MDPI and/or the editor(s) disclaim responsibility for any injury to people or property resulting from any ideas, methods, instructions or products referred to in the content.